Quaternary Science Reviews 186 (2018) 225–235

Contents lists available at ScienceDirect

Quaternary Science Reviews

journal homepage: www.elsevier.com/locate/quascirev

A leaf wax biomarker record of early Pleistocene hydroclimate from West Turkana, Kenya

R.L. Lupien [a, *], J.M. Russell [a], C. Feibel [b], C. Beck [c, b], I. Castañeda [d], A. Deino [e], A.S. Cohen [f]

[a] Brown University, Department of Earth, Environment, and Planetary Sciences, 324 Brook Street, Providence, RI, 02906, USA
[b] Rutgers University, Department of Earth and Planetary Sciences, 610 Taylor Road, Piscataway, NJ, 08854, USA
[c] Hamilton College, Department of Geosciences, 198 College Hill Road, Clinton, NY, 13323, USA
[d] University of Massachusetts Amherst, Department of Geosciences, 627 North Pleasant Street, Amherst, MA, 01002, USA
[e] Berkeley Geochronology Center, 2455 Ridge Road, Berkeley, CA, 94709, USA
[f] University of Arizona, Department of Geosciences, 1040 East 4th Street, Tucson, AZ, 85721, USA

ARTICLE INFO

Article history:
Received 2 August 2017
Received in revised form
13 January 2018
Accepted 5 March 2018

Keywords:
Human evolution
Paleoclimatology
Pleistocene
Continental biomarkers
Organic geochemistry
Hydrogen isotopes
East Africa
Turkana basin

ABSTRACT

Climate is thought to play a critical role in human evolution; however, this hypothesis is difficult to test due to a lack of long, high-quality paleoclimate records from key hominin fossil locales. To address this issue, we analyzed organic geochemical indicators of climate in a drill core from West Turkana, Kenya that spans ~1.9–1.4 Ma, an interval that includes several important hominin evolutionary transitions. We analyzed the hydrogen isotopic composition of terrestrial plant waxes (δD_{wax}) to reconstruct orbital-timescale changes in regional hydrology and their relationship with global climate forcings and the hominin fossil record. Our data indicate little change in the long-term mean hydroclimate during this interval, in contrast to inferred changes in the level of Lake Turkana, suggesting that lake level may be responding dominantly to deltaic progradation or tectonically-driven changes in basin configuration as opposed to hydroclimate. Time-series spectral analyses of the isotopic data reveal strong precession-band (21 kyr) periodicity, indicating that regional hydroclimate was strongly affected by changes in insolation. We observe an interval of particularly high-amplitude hydrologic variation at ~1.7 Ma, which occurs during a time of high orbital eccentricity hence large changes in processionally-driven insolation amplitude. This interval overlaps with multiple hominin species turnovers, the appearance of new stone tool technology, and hominin dispersal out of Africa, supporting the notion that climate variability played an important role in hominin evolution.

© 2018 Elsevier Ltd. All rights reserved.

1. Introduction

Understanding the link between human evolution and environmental change is one of the most enduring challenges in the Earth Sciences. An early idea, dubbed the savannah hypothesis (Dart, 1925), posited that global cooling during the Plio-Pleistocene led to gradual drying of Africa, which in turn altered vegetation structure from closed-canopy forest to open savannah, and triggered anatomical and behavioral changes in early hominins (Cerling, 1992; Cerling and Hay, 1986; deMenocal, 1995; Feakins et al., 2005; Levin et al., 2011; Uno et al., 2016b). Although there is clear evidence for the development of drier conditions in Africa over the Plio-Pleistocene from paleoceanographic (deMenocal, 2004) and soil carbonate (Levin et al., 2004) records, it has proven difficult to associate individual transitions in specific locales in the hominin fossil records with these gradual, continental-scale environmental changes. More recent hypotheses suggest much more complex connections between hominins and their environment that account for abrupt changes and high variability evident in African paleoclimate records. The turnover pulse hypothesis (Vrba, 1980, 1989, 1995) suggests that rapid shifts between environmental extremes, caused by climatic or geologic events, force evolutionary changes, whereas the variability selection hypothesis posits that changes in environmental variability select for traits that lead to adaptability in hominin lineages to cope with highly variable landscapes (Bobe and Behrensmeyer, 2004; Grove, 2014, 2015; Maslin et al., 2014; Maslin and Trauth, 2009; Potts, 1996, 1998a, b; Potts and Faith, 2015; Trauth et al., 2010). Each of these hypotheses makes a specific prediction about the timing, rate, or pattern of

* Corresponding author.
E-mail address: rachel_lupien@brown.edu (R.L. Lupien).

https://doi.org/10.1016/j.quascirev.2018.03.012
0277-3791/© 2018 Elsevier Ltd. All rights reserved.

African environmental change, which would be best tested against paleoenvironmental records obtained from the basins where our hominin ancestors lived.

African climate change during the Plio-Pleistocene occurred in the context of large changes in global climate boundary conditions and forcing. Over the course of the Pleistocene, global climate cooled and the northern high latitude ice sheets expanded and oscillated at 41 and 100 kyr periodicities (Lisiecki and Raymo, 2005; Zachos et al., 2001). Closure of the Indonesian seaway could have induced African aridification as early as 3–4 million years ago (Cane and Molnar, 2001) and the enhancement of tropical latitudinal temperature gradients (Walker Circulation) at ~1.7 Ma (Ravelo et al., 2004) may have driven changes in African rainfall (Brierley et al., 2009). These influences, as well as cyclic changes in insolation driven by orbital precession, are all thought to modulate African rainfall (Brierley et al., 2009; deMenocal, 2004; Pokras and Mix, 1987). Paleoclimate reconstructions from marine sequences, including inferences of tropical sea surface temperature (SST) and African dust accumulation, document environmental fluctuations that appear to be in phase with northern hemisphere glaciation (NHG; deMenocal, 1995; Herbert et al., 2010). On the other hand, changes in the magnitude of tropical insolation resulting from Earth-orbital precession, may strongly influence African monsoons; many paleoclimate records show strong ~21 kyr periodicity, particularly in North and East Africa (Hilgen, 1991; Joordens et al., 2011; Kingston et al., 2007; Lourens et al., 1996; Maslin et al., 2014; Maslin and Trauth, 2009; Rossignol-Strick, 1985; Trauth et al., 2007). Unfortunately, existing terrestrial records are generally of low temporal resolution, and are often short and discontinuous, and are therefore unable to determine the large-scale controls on tropical African rainfall. In contrast, marine sediment cores provide long, continuous climate histories but generally record environmental changes at the continental scale, thus ill-suited to investigate the environmental history of the specific regions in which hominins evolved.

The Hominin Sites and Paleolakes Drilling Project (HSPDP) is an international collaboration that drilled long cores from six paleolakes in the East African Rift System (EARS) to characterize the paleoenvironments in which our human ancestors lived and evolved (Campisano et al., 2017; Cohen et al., 2009, 2016). Because of fast sedimentation rates in these lacustrine basins, and a more limited sediment source area than offshore marine sites, these cores can provide environmental records with high temporal and spatial resolution to test the predictions of theories linking human evolution to climate change. Here, we present records of climate from the West Turkana Basin, Kenya, based on deuterium (D) to hydrogen (H) isotope ratios from terrestrial plant waxes (δD_{wax}) preserved in HSPDP core HSPDP-WTK13-1A (hereafter WTK13). The Turkana Basin has been well-characterized geologically and is the source of ~500 hominin fossil discoveries and contains over 100 archaeological sites (Wood and Leakey, 2011), including the earliest and most complete skeletons of *Homo rudolfensis* and *H. erectus* and Acheulean stone tools (advanced hand axes; Lepre et al., 2011). Our record spans almost 500 kyr of the early Pleistocene, from 1.86 to 1.37 Ma, which witnessed a critical evolutionary transition marked by the demise of *H. habilis* and *H. rudolfensis* and the rise of *H. erectus*. Our δD_{wax} record provides new insight into the patterns and causes of climate change during this important time window.

2. Regional setting

The Turkana Basin is comprised of half-graben subsiding blocks, extends from central Kenya northward into southern Ethiopia in the eastern branch of the EARS, and today houses Lake Turkana, the world's largest desert lake (Feibel, 2011). It receives less than 200 mm of precipitation annually, with rainfall occurring in two rainy seasons associated with the seasonal migration of the Intertropical Convergence Zone (ITCZ) across the equator (Yang et al., 2015; Yuretich and Cerling, 1983). The Congo Air Boundary (CAB), which separates Atlantic and Indian Ocean-derived moisture sources, currently lies well to the west of Lake Turkana over Central Africa. Modern Lake Turkana is fed mostly by the Omo River, which forms a large delta at the northern end of the lake. During the early Pleistocene, Lake Lorenyang filled much of the Turkana Basin (Fig. 1), with numerous fossils, including hominins, preserved in its lake-marginal and terrestrial sediment fill (Harris et al., 1988; Roche et al., 2003). Because of ongoing rifting, sediment deposition is and was highly dynamic, and was also impacted by extensive volcanism, fluctuating deltaic systems, and dramatic lake level changes (Feibel, 2011; Feibel et al., 1989). We focus on paleolake sediments drilled from west of modern Lake Turkana in the Nachukui Formation (~4°N, ~36°E; Fig. 1).

3. Material and methods

Core WTK13 was taken in 2013 from a borehole oriented at 10° from vertical, and achieved 94.1% recovery (Cohen et al., 2016). The bottom ~155 m of the 216.47 m core is mostly comprised of dark green fine siltstones, signifying deep lake environments, intermittently overprinted by weakly developed paleosols. Sediments above 61 m below the surface (mbs) are generally coarser red silts and sands, signifying a shift to shallower, more oxidizing lacustrine and deltaic environments. We determined a chronology for WTK13

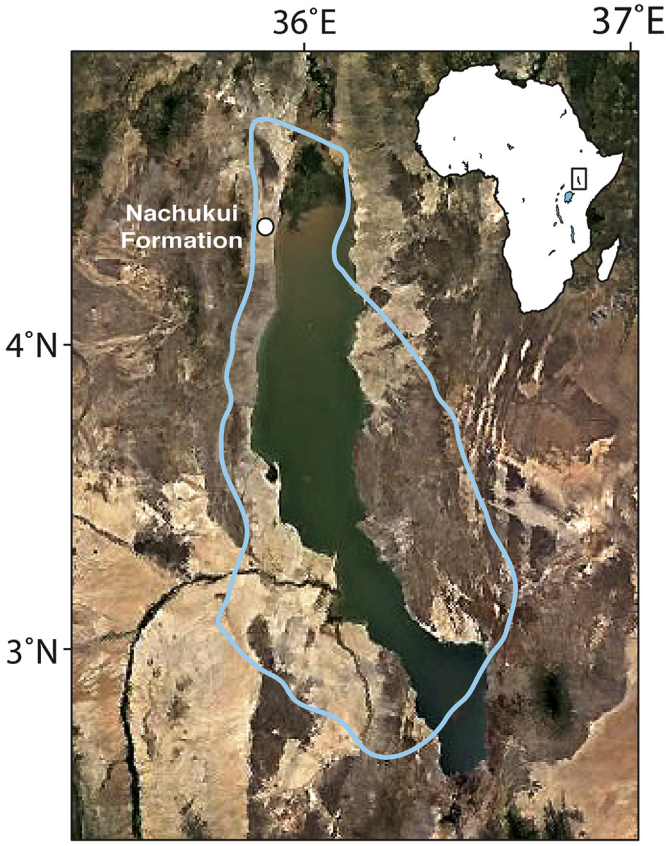

Fig. 1. The present-day Lake Turkana Basin (Google Earth) with paleolake Lorenyang ~1.9 Ma outlined in blue (Brown and Feibel (1991). The location of core WTK13 that sampled the Nachukui Formation is indicated by a white circle. (For interpretation of the references to color in this figure legend, the reader is referred to the Web version of this article.)

based upon correlation of tephras in the core with tephras of known age in the region, direct $^{40}Ar/^{39}Ar$ dating of a new tephra discovered in the core, and paleomagnetic reversal stratigraphy reported in Sier et al. (2017).

Plants produce waxy cuticles on their surfaces to prevent evaporation (Eglinton and Hamilton, 1967). These waxes may be ablated and transported by wind or water to lake sediments, where they are preserved over geological time. These epicuticular waxes include long-chain *n*-alkanoic acids, which we used to evaluate paleohydrologic changes. Samples of 2–5.5 cm thickness (mean 2.9 cm, or ~70 years) were taken every ~1 m throughout WTK13, providing an average sampling resolution of ~3 kyr. Procedures for lipid extraction, purification, and isotopic analyses are based upon those of Konecky et al. (2011). Lipids were extracted from freeze-dried and homogenized bulk sediment using a DIONEX Accelerated Solvent Extractor 350 with dichloromethane:methanol (9:1). The lipids were separated into neutral and acid fractions over an aminopropylsilyl gel column using dichloromethane:isopropanol (2:1) and ether:acetic acid (24:1), respectively. The acids were methylated using acidified methanol, and the resulting fatty acid methyl ethers (FAMEs) were purified via silica gel column chromatography. Relative abundances of the FAMEs were quantified using an Agilent 6890 gas chromatograph (GC) equipped with a HP1-MS column (30 m × 0.25 mm × 0.25 μm) and flame ionization detector. 159 and 198 samples contained compound concentrations adequate for hydrogen (δD_{wax}) and carbon ($\delta^{13}C_{wax}$) isotopic analysis, respectively, and were analyzed at Brown University. Hydrogen isotopes were measured on an Agilent 6890 GC, equipped with HP1-MS column (30 m × 0.32 mm × 0.25 μm), coupled to a Thermo Delta Plus XL isotope ratio mass spectrometer (IRMS) with a reactor temperature of 1445 °C. D/H ratios were measured using H_2 as an internal standard with He as the carrier gas, and corrected using a FAMEs standard, run every seventh injection. Isotopic analyses of the standard had a standard deviation (σ) of 2.4‰. The H_3^+ factor was 2.43 ($1\sigma = 0.14$) throughout these analyses. Measured isotopic values were accepted if the voltage was between 2.5 and 8 V. Carbon isotopes were measured on an Agilent 6890 GC, equipped with HP1-MS column (30 m × 0.25 mm × 0.10 μm) coupled to a Thermo Delta V Plus IRMS with a reactor at 1100 °C. For $^{13}C/^{12}C$ ratios, the IRMS was run with CO_2 as the internal standard, with a FAMEs standard deviation of 1.1‰. All measurements were corrected for the isotopic composition of the added methyl group, where $\delta D_{MeOH} = -123.7‰$ and $\delta^{13}C_{MeOH} = -36.52‰$ (Tierney et al., 2011).

The hydrogen isotopic ratio was measured on most samples in triplicate and carbon isotope ratios in duplicate where possible; however, small sample sizes dictated that some samples were measured using single injections. Samples measured in triplicate had an average standard deviation of 1.33‰ and a maximum of 4.49‰ for δD_{wax}, whereas samples run in duplicate had an average inter-sample difference of 1.70‰ and a maximum of 8.08‰. Carbon isotope ratios were measured in duplicate on each sample with an average inter-sample difference of 0.13‰. We found one outlier in δD_{wax} at 48.36 mbs, which was measured as a single injection due to limited sample amount, and this sample was excluded from further discussion and analysis. Similarly, one outlier in $\delta^{13}C_{wax}$ exists at 61.38 mbs and this sample was also excluded from further discussion. We report δD_{wax} and δD of precipitation (δD_{precip}) relative to Vienna standard mean ocean water (VSMOW) and $\delta^{13}C_{wax}$ relative to Pee Dee belemnite (PDB) in per mil (‰) notation.

Different types of plants (e.g. C_3 trees versus C_4 grasses) fractionate hydrogen to different degrees during leaf wax synthesis as a result of differing metabolic pathways and plant physiologies. This causes different apparent fractionations between leaf waxes and precipitation ($\varepsilon_{wax\text{-}P}$), which can affect paleoclimate records based on δD_{wax} if vegetation changes (Sachse et al., 2012). We calculated a 'vegetation correction' based upon $\delta^{13}C_{wax}$ values to correct δD_{wax} for these differences, as previously described by Konecky et al. (2016). We use $\delta^{13}C_{wax}$ endmember values for C_3 and C_4 plant types previously described from the Nachukui outcrop (Uno et al., 2016b), in which the $\delta^{13}C$ of *n*-C_{30} acids is −32.9‰ for the C_3 endmember and the $\delta^{13}C$ of *n*-C_{30} acid is −19.0‰ for the C_4 end member. We adjust these values by +2.2‰ to account for observed differences between *n*-C_{30} and *n*-C_{28} acids (Gao et al., 2014), thereby using −30.7‰ and −16.8‰ as the C_3 and C_4 endmembers. Samples with $\delta^{13}C_{wax}$ values more enriched than this C_4 endmember value ($n = 10$) are treated as 100% C_4. After applying this C_3/C_4 mixing model to our $\delta^{13}C_{wax}$ data, we then applied $\varepsilon_{wax\text{-}P}$ values of −112.8‰ and −124.5‰ for C_3 and C_4 vegetation with a 25‰ correction for C_{27} *n*-alkane to C_{28} *n*-acid (Chikaraishi and Naraoka, 2007; Konecky et al., 2016; Sachse et al., 2012) to correct for 'vegetation effects' on δD_{wax} and estimate δD_{precip} (Fig. 2).

Because of limited sample size, not all samples could be measured for both δD_{wax} and $\delta^{13}C_{wax}$, so this 'vegetation correction' limited the number of δD_{precip} data points. As a result, and because δD_{precip} and δD_{wax} are strikingly similar (Fig. 2), our discussion and analysis below relies largely on δD_{wax}. The $\delta^{13}C_{wax}$ from WTK13 shows complex relationships with δD_{wax}, including both in and out of phase relationships at different core intervals. The nature of the relationship between $\delta^{13}C_{wax}$ and δD_{wax} can be complicated in desert environments such as Lake Turkana, where $\delta^{13}C_{wax}$ can have a more complex relationship with climate than is typically assumed. One explanation could be that C_4 grassland expansion occurs at the expense of more xerophytic vegetation in response to wetter conditions, which has been previously documented (Achyuthan et al., 2007; Ivory and Russell, 2016; Thomas et al., 2014). Alternatively, African vegetation is known to respond to a variety of climate and environmental forcings, including precipitation seasonality, fire, and other drivers not recorded by our δD_{wax} data (Ivory and Russell, 2016). Full analyses of the $\delta^{13}C_{wax}$ record will be presented in a future paper that incorporates other paleoecological indicators.

Statistical analyses were performed on δD_{wax} to characterize the patterns of past climate change in the Turkana Basin. Spectral analyses of detrended δD_{wax} using the Lomb-Scargle method were used to identify significant frequencies of variability (Trauth, 2015). A wavelet evolutionary spectrum (performed on linearly resampled δD_{wax}) was used to determine how spectral properties changed through time. We also calculated changes in the variance of δD_{wax} and other data within a moving ~50 kyr window to estimate the timing of changes in the amplitude of variability within the record. The top 60 m of the core have lower sampling resolution due to low lipid concentrations, and because of very low sample resolution between ~1.50 (60 mbs) and ~1.43 Ma (46 mbs), spectral and wavelet analyses were only performed on the deeper section of core (1.86–1.50 Ma).

4. Results and interpretive framework

An age model for WTK13 was developed using tephrocorrelation of the Chari Tuff (1.388 Ma), Etirr Tuff (1.45 Ma), and Ebei Tuff (1.48 Ma) (Table S2; Fig. S2), an $^{40}Ar/^{39}Ar$ single-crystal sanidine age measured on a previously unknown tuff (1.497 Ma), paleomagnetic identification of the top of the Olduvai Subchron (1.778 Ma; Sier et al., 2017), as well as the inferred depth of the KBS tuff. The KBS tuff (1.875 Ma; Feibel et al., 1989) is found throughout the region, but is not present in WTK13. Based on correlations to outcrops and appropriate sedimentation rates, we estimate that it lies very close to the base of the core; the bottom age of the core was therefore estimated at 1.870 Ma. Due to the relatively small

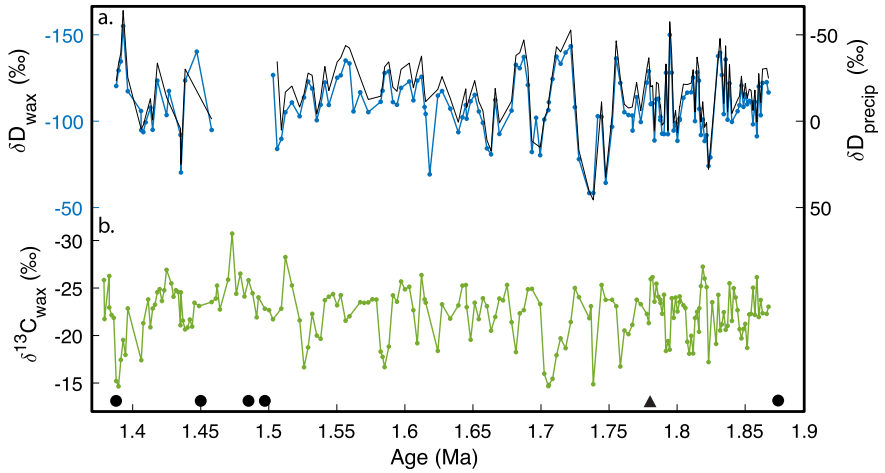

Fig. 2. a) δD_{precip} in black is plotted with measured δD_{wax} in blue. b) The $\delta^{13}C_{wax}$ (green) was used to correct for 'vegetation effects' on δD_{wax} as outlined by Konecky et al. (2016). Black circles represent age constraints based on tephrochronology and the black triangle represents age constraint based on magnetostratigraphy. (For interpretation of the references to color in this figure legend, the reader is referred to the Web version of this article.)

number of chronostratigraphic control points to develop our age model, we employ a simple three-segment linear regression encompassing the core. The segments yield sedimentation rates of 58.3, 33.3, and 71.2 cm/kyr from top to bottom (Table S1; Fig. S1). Additional information about the age model is provided in the supplementary material.

C_{26}, C_{28}, and C_{30} *n*-acids were the most abundant long-chain wax homologues found in the West Turkana samples. These long-chain waxes are primarily derived from higher terrestrial plants, rather than aquatic sources (Eglinton and Hamilton, 1967; Sachse et al., 2012; Volkman et al., 1998), and their δD_{wax} values were strongly positively correlated (C_{28}-C_{26} $r^2 = 0.84$; C_{28}-C_{30} $r^2 = 0.75$; C_{26}-C_{30} $r^2 = 0.82$) demonstrating that these waxes are derived from a common source (i.e. higher plants). Here we report the δD_{wax} of C_{28} *n*-alkanoic acid because of its high abundance in our samples, which resulted in a lower analytical error and more frequent measurements in the core.

The δD_{wax} of *n*-C_{28} ranges between −58 and −181‰ and averages −110‰ (Fig. 3). Application of the $\delta^{13}C_{wax}$ vegetation correction to δD_{wax} generates a δD_{precip} record that is very similar to the δD_{wax} record, with an average δD_{precip} of −17‰ and a range of −110‰ (Fig. 3). The $\delta^{13}C_{wax}$ averages −22‰, and the values range from −31 to −15‰, similar to the full range of observed $\delta^{13}C_{wax}$ of C_3 to C_4 plants (Chikaraishi and Naraoka, 2007).

The Average Chain Length (ACL) of the *n*-alkanoic acids (C_{16}-C_{32}) is 27.6, similar to modern East African lake sediment samples (Garcin et al., 2012; Uno et al., 2016a; Vogts et al., 2009). The Carbon Preference Index (CPI C_{16}-C_{32}; Bray and Evans, 1961) values averaged 5.1 in our samples. Modern plant material generally has *n*-alkanoic acid CPI values of at least 6, whereas highly degraded hydrocarbons (up to oil) have values of 1. The CPI values observed in WTK13 are thus well above those of highly degraded organic matter and indicate generally good preservation of *n*-alkanoic acids. Samples from the coarser-grained, oxidized upper ~60 m of core have lower CPI values (average of 2.67), reflecting more degraded leaf waxes. However, in this interval, and throughout our core, CPI and δD_{wax} values are uncorrelated ($n = 159$, $r^2 = 4.9 \times 10^{-6}$), suggesting degradation has little effect on the isotopic composition of these waxes. ACL and δD_{wax} are also not correlated ($n = 159$, $r^2 = 0.02$), indicating that any changes in wax source do not strongly affect their isotopic composition. Thus, we interpret the δD_{wax} measurements to represent δD_{wax} at the time of

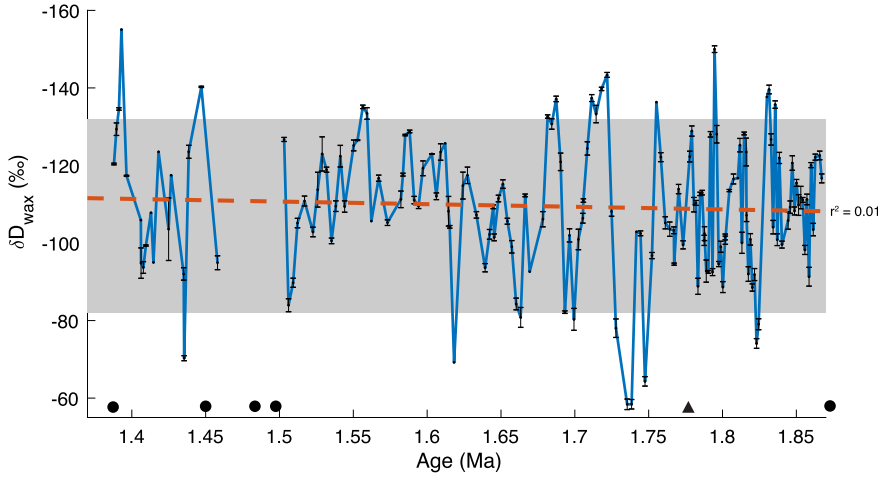

Fig. 3. δD_{wax} from core WTK13 from Lake Turkana, Kenya. The orange dotted line is a least-squares linear regression of the δD_{wax} data on time. The grey region denotes the range of δD_{wax} variation from the last glacial maximum (~20 kyr BP) to the present for comparison (Morrissey, 2014). Age constraints as in Fig. 2. (For interpretation of the references to color in this figure legend, the reader is referred to the Web version of this article.)

deposition.

Previous studies have shown that δD_{wax} is strongly correlated with mean annual δD_{precip} (Garcin et al., 2012; Hou et al., 2008; Polissar and Freeman, 2010; Sachse et al., 2004; Schefuβ et al., 2005). In the tropics, the 'amount effect' is the dominant influence on δD_{precip} variation (Dansgaard, 1964; Rozanski et al., 1993; Scholl et al., 2009; Vuille et al., 2005). The amount effect describes the inverse correlation between rainfall amount and isotopic composition, and is driven by removal of isotopically enriched vapor during condensation and reduced evaporation of raindrops falling through a humid atmosphere. Other factors such as moisture source, transport distance, temperature, and an array of cloud-scale processes may also influence δD_{precip} (Dansgaard, 1964; Konecky et al., 2011; Vuille et al., 2005). For instance, in tropical East Africa, CAB movement could alter the balance between Indian Ocean-sourced and Atlantic Ocean-sourced moisture, which differ isotopically due to differing transport pathways and evapotranspiration histories (Costa et al., 2014; Joseph et al., 1992; Levin et al., 2009; Sonntag et al., 1979). Although we generally assume that the amount effect is the primary influence on our δD_{precip} record, the potential influence of these processes will be discussed below.

5. Discussion: Paleoclimate of the Turkana Basin

5.1. Orbital-scale controls on early Pleistocene African climate

Many records indicate strong influences of high latitude climate on African paleoclimate and paleoenvironments. Marine records of North African dust flux have documented transitions from precession- to obliquity- to eccentricity-dominated variability during the Plio-Pleistocene that match the frequency and timing of high latitude glacial cycles, suggesting strong controls of global ice volume and high latitude climate on North African aridity (deMenocal, 1995). Although statistical analyses have called these results into question (Trauth et al., 2009) and other marine dust records present conflicting climate signals (e.g. Larrasoaña et al., 2003), records of tropical Indian Ocean SST, which should impact moisture availability and rainfall patterns on the African continent (Nicholson, 1996), also show strong correspondence to global ice volume during the Plio-Pleistocene (Herbert et al., 2010). Indeed, there are hundreds of records from tropical Africa that indicate drying during the last glacial maximum (~21 Ka) relative to the present, demonstrating the importance of global climate boundary conditions associated with glaciation to African climate in recent time (Gasse, 2000). Northern high latitude glaciation could affect African rainfall via many pathways, such as changes in interhemispheric temperature gradients and orographic forcing by the ice sheets that alter the position of the tropical rain belt (e.g. Shanahan et al., 2015). Alternatively, these correlations could indicate links between high latitude climate and tropical African rainfall through tropical SSTs and African continental temperature, both of which are likely controlled by atmospheric pCO_2 variation, which could alter precipitation rates within the tropical rainbelt itself (Otto-Bliesner et al., 2014). Thus, East African rainfall, ITCZ location, and monsoon strength can vary in response to forcing from the high latitude ice sheets and atmospheric greenhouse gas boundary conditions.

Other East African paleoclimate records point to a dominant role for changes in seasonal insolation in the tropics in driving the African monsoon. Mediterranean sapropel deposits, which record freshwater runoff from North Africa, show strong signals from eccentricity-modulated precession, with intervals of strong summer insolation in the northern tropics linked to high rainfall and runoff (Lourens et al., 1996; Rossignol-Strick, 1985). Geochemical reconstructions from Mediterranean deposits agree with this interpretation of a precession-band driver of hydroclimate and vegetation (Rose et al., 2016). Some reconstructions from the EARS have identified repeated cycles of deep and shallow lake levels that show evidence of insolation forcing from orbital precession (Kingston et al., 2007; Lepre et al., 2007; Shultz and Maslin, 2013). This includes reconstructions from West Turkana, where an isotopic record of chemical weathering shows strong ~21 kyr cyclicity from orbital precession between ~1.85 and 2 Ma (Joordens et al., 2011), slightly older than the base of the WTK13 core. Although lake levels may be influenced by tectonic basin activity (Carroll and Bohacs, 1999; Lepre, 2014), there are key questions as to whether the large-scale patterns of lake evolution within the EARS are driven by changes in fault activity or climate (Trauth et al., 2007). Astronomically-driven changes in seasonal insolation, rather than glacial-interglacial cycles, may be the primary driver of East African paleoclimate.

Our age model is anchored by a limited number of data points and therefore precludes us from examining the timing of specific precession-scale events in the WTK13 record. However, Lomb-Scargle time series spectral analysis of our δD_{wax} data shows strong spectral density (Fig. 4a) at both 41 kyr, similar to orbital obliquity, and ~18 kyr, which is similar to, but slightly shorter than, orbital precession. A wavelet analysis of Turkana δD_{wax} confirms these signals, indicating relatively persistent high frequency variation from ~18 to 20 kyr. We also observe high spectral density during a shorter interval centered at ~1.71 Ma (133 mbs) at a period of ~38 kyr (Fig. 4b). Peaks in spectral density, at ~18 kyr in particular, are noisy (Fig. 4a), potentially because of variable sampling resolution or age model inaccuracies. However, the presence of significant periodicities at ~38–41 and ~18–20 kyr suggests the influence of orbital obliquity (41 kyr) and precession (21 kyr) in the WTK13 record.

The presence of a δD_{wax} signal compatible with orbital precession, during a period in which glacial-interglacial cycles were predominantly every 41 kyr, supports previous suggestions of the importance of insolation forcing of the African monsoon (e.g. Lourens et al., 1996; Rose et al., 2016; Rossignol-Strick, 1985), including reconstructions from within the Turkana Basin itself (Joordens et al., 2011). In more recent times, the water level of Lake Turkana has also been demonstrated to vary with insolation (Butzer et al., 1972; Garcin et al., 2012; Morrissey and Scholz, 2014; Owen et al., 1982), suggesting that orbital forcing is a strong influence on regional hydroclimate. Our record confirms and extends this signal over much of the early Pleistocene.

We also observe a brief interval (~1.76–1.66 Ma) during which δD_{wax} varies at ~32–40 kyr, near the pace of orbital obliquity. As tropical insolation varies only slightly due to obliquity, this periodicity has typically been interpreted to reflect a high northern latitude influence on African hydrology (deMenocal, 1995). Both tropical SST and global ice volume show strong obliquity variation during this time period (Herbert et al., 2010; Lisiecki and Raymo, 2005), and it is possible that the early Pleistocene obliquity-band variability observed in West Turkana signifies a local response to tropical SSTs or remote responses to changing high latitude glaciation. However, neither the benthic $\delta^{18}O$ record of ice volume ($r^2 = 0.04$, $p = 0.02$) nor western Indian Ocean SSTs ($r^2 = 0.03$, $p = 0.04$) are strongly correlated with our δD_{wax} record during this time interval (Fig. 5), and the mechanisms that would link obliquity, ice volume, and tropical SSTs with East African rainfall during only the 1.8–1.7 Ma interval are unclear.

There are several factors that lead us to question whether the obliquity signal is robust. There is relatively low sampling resolution in our record during this interval because of low core recovery, with up to 8 kyr between samples. This may account for a loss of high-frequency variation, i.e. weakened precession-band variability

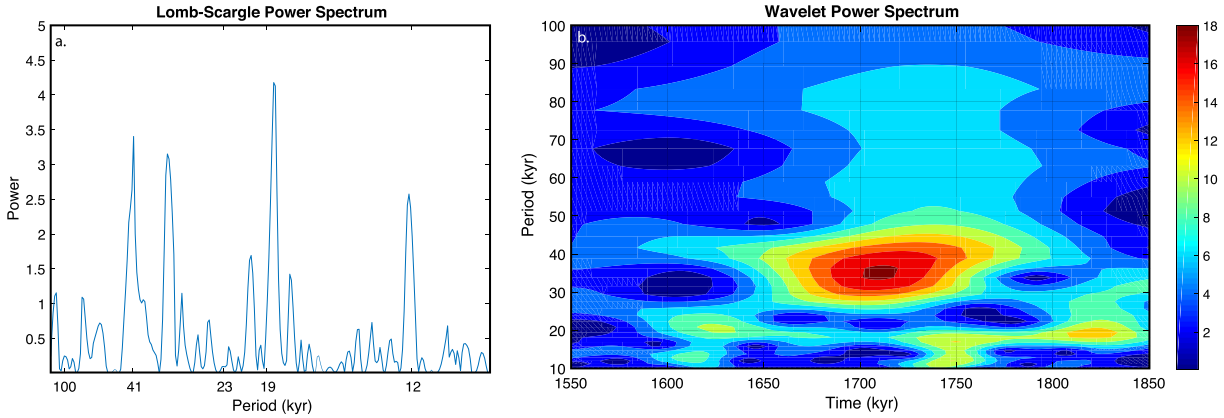

Fig. 4. Time series spectral analyses of West Turkana δD_{wax}. a) Lomb Scargle spectral analysis. b) Wavelet evolutionary spectrum, which shows time versus periodicity with warmer colors signifying higher spectral density. (For interpretation of the references to color in this figure legend, the reader is referred to the Web version of this article.)

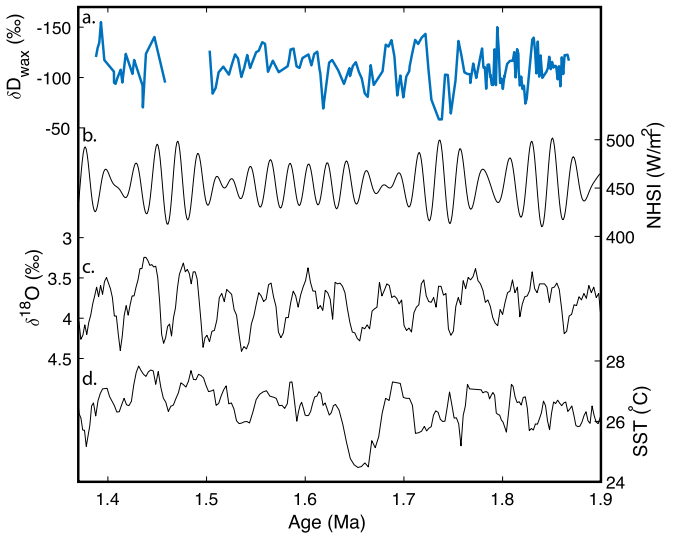

Fig. 5. Early Pleistocene African paleoclimate records and climate forcings plotted with warmer and/or wetter conditions up. a) WTK13 δD_{wax} from this study. b) NH summer insolation from 20°N (Laskar et al., 2004). c) Benthic foraminifera $\delta^{18}O$ record of global ice volume (Lisiecki and Raymo, 2005). d) Arabian Sea alkenone-based SST reconstruction from ODP 722 (Herbert et al., 2010).

(Fig. 4b). Additionally, the ~32–40 kyr periodicity is largely driven by three pronounced δD_{wax} minima that occur during this interval with a spacing of ~35 kyr. It is also possible that sedimentation rates changed during this time interval, but our limited number of age control points precludes testing this possibility. To examine the potential that the age model and/or low sampling resolution may have affected our spectral results, we tuned the δD_{wax} record to June 21st mean insolation at 20°N (the latitude at which insolation controls the tropical monsoon system), as was previously done for older sediments in the Turkana Basin (Fig. 6a; Joordens et al., 2011). This tuning requires adjusting the ages of individual data points within this interval by an average of only 2.2 kyr, and after tuning, Lomb Scargle and wavelet spectral analyses detect a dominant ~21 kyr periodicity with minimal 41 kyr variation (Fig. 6b). We do not imply that this tuning and age model are necessarily correct; however, this analysis shows that the obliquity signal can be completely removed with very slight adjustments of the age model and δD_{wax} record, suggesting that the presence of this period depends strongly on the age model. We therefore suggest that insolation forcing at the precession band is likely the dominant control on regional Turkana Basin hydroclimate during the early Pleistocene.

5.2. Long-term trends in Turkana paleohydrology from 1.9 to 1.4 Ma

Many records indicate that East Africa has become progressively drier through the Plio-Pleistocene. This scenario is the foundation for the savannah hypothesis (Dart, 1925), and evidence for a shift from a warm, wet Pliocene to a cool, dry late Pleistocene is evident in many records of African climate including soil carbonate isotopes, faunal assemblages, and leaf wax biomarker records from marine sediment (Cerling, 1992; Cerling and Hay, 1986; Uno et al., 2016b). However, drying over the Plio-Pleistocene was not necessarily a continuous process, and not all 500 kyr (the amount of time spanned by WTK13) intervals within the Plio-Pleistocene exhibit a drying trend. The early Pleistocene in West Turkana presents an interesting case to investigate long-term directional trends in African climate. During the early Pleistocene, Lake Lorenyang, Turkana's longest-lived lake, expanded, and eventually gave way to more discontinuous fluvial deposits (Feibel, 2011). Although this transition could suggest a drying climate, tectonically-driven changes in basin configuration, and outlet position or simply deltaic progradation in the absence of any changing climate or tectonic forcing could complicate the climatic interpretation of this apparent lake regression.

The WTK13 core straddles this transition, and its lithology indicates a shift from the deep lake facies of Lake Lorenyang to the shallow lake and fluvial sediments of the Omo Group. Interestingly, however, our δD_{wax} record shows no statistically significant trend nor shift in long-term mean over this ~500 kyr span (Fig. 2). Similarly, we see no shift in $\delta^{13}C_{wax}$, suggesting little to no change in vegetation type driven by changes in rainfall or moisture balance. Although this is surprising in light of the lithologic evidence for lake level regression and faunal evidence for ecosystem changes at this time, our result is consistent with oxygen isotopic analyses of tooth enamel in the Turkana Basin (Blumenthal et al., 2017) as well as Sr-isotopic analyses of basin hydrology spanning the interval from 2 to 1.85 Ma (Joordens et al., 2011). Moreover, key drivers of East African climate, namely local mean summer insolation, global ice volume, and Indian Ocean SSTs, also do not show significant trends during this time window that would have forced large directional changes in African climate (Fig. 5). We do observe that the average δD_{wax} in our record is ~25‰ more depleted than waxes deposited in recent (late Holocene) sediments from modern-day Lake Turkana

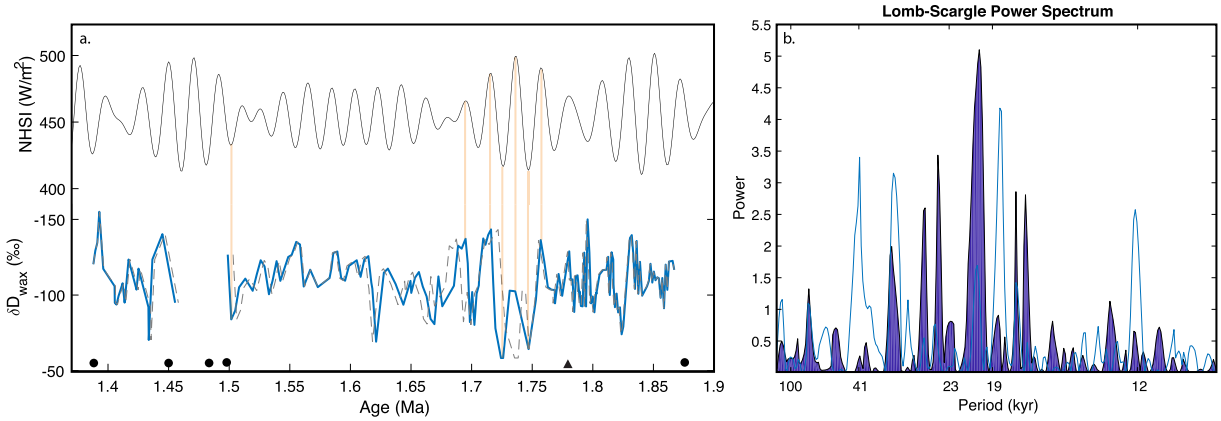

Fig. 6. Results of tuning δD_{wax} to solar insolation at 20°N. a) δD_{wax} (blue) tuned to June 21st solar insolation at 20°N (black) with few tie lines plotted in orange. The original (untuned) δD_{wax} record is in dashed grey to show the minor effects of tuning. b) The Lomb Scargle spectral analysis of tuned δD_{wax} (purple area) overtop Lomb Scargle spectral analysis of untuned δD_{wax} (blue line). Age constraints as in Fig. 2. (For interpretation of the references to color in this figure legend, the reader is referred to the Web version of this article.)

(Morrissey, 2014), suggesting Turkana was generally wetter during the early Pleistocene than in the present. This is in keeping with the globally cooler and likely locally drier conditions that developed from the early to late Pleistocene.

Rather, our data suggest that the shift in sediment facies in the WTK13 core is driven by changes in delta progradation, fault motion, subsidence, outlet level, or similar processes that influenced Turkana's depositional environments. Our δD_{wax} record primarily responds to changes in atmospheric circulation and processes governing rainfall, and should therefore be less sensitive than sediment lithology to local, perhaps tectonically-driven changes in basin morphology. It is possible that δD_{wax} was influenced by processes other than the amount effect on this timescale, such as changes in moisture source or transport pathway. However, we would expect to see some shift in δD_{wax} driven by atmospheric circulation changes if the lake level regression were related to regional precipitation, unless the effects of changes in moisture source, transport, and other processes perfectly balanced the effects of changes in precipitation amount on δD_{wax}. Moreover, the $\delta^{13}C_{wax}$ record from West Turkana shows no trend over the length of our record, implying that mean vegetation composition changed little over this ~500 kyr time period. This is somewhat surprising in light of the development of large deltaic complexes in the upper part of the core, which might be expected to alter local vegetation and affect $\delta^{13}C_{wax}$. However, because plant waxes can be sourced from large areas (e.g. the Turkana Basin), the influences of local sedimentary environments may be weak. It is alternatively possible that there were substantial changes in vegetation structure that are not recorded in our $\delta^{13}C_{wax}$ record, such as changes of plant types within C_3 and C_4 groups. Whatever the case may be, taken together, our data argue for very limited change in the mean precipitation of the Turkana Basin during the interval from 1.9 to 1.4 Ma.

5.3. High amplitude climate variation from 1.8 to 1.7 Ma

Mediterranean sapropel and geochemical records indicate that both the timing and amplitude of wet phases in North Africa are tied to orbital precession and the amplitude of insolation change in summer, which is paced by eccentricity modulation of precession (Lourens et al., 1996; Rose et al., 2016; Rossignol-Strick, 1985). Generally, terrestrial records are too short to test this finding; however, deep paleolake intervals in the Baringo Basin appear to be restricted to intervals of high eccentricity (Deino et al., 2006; Kingston et al., 2007). Maslin et al. (2014) suggest that these "deep lake intervals" are synchronized across East Africa and develop during intervals of highly variable insolation (i.e. high eccentricity; Maslin et al., 2014; Trauth et al., 2005; Trauth et al., 2007). However, not all intervals of high eccentricity during the Plio-Pleistocene lead to deep lake intervals, and many of these deep lake intervals coincide with the timing of global climate transitions, such as wet conditions during the onset of the NHG captured by the Baringo Basin record (Kingston et al., 2007). Moreover, although lake highstand deposits and sapropels can record much wetter conditions during insolation maxima, lake depth records derived from outcrops exhibit a binary response to climate (i.e. lake vs. no lake), making it difficult to investigate the extent of aridity during insolation minima. Thus, our understanding of changes in climate variability in response to varying insolation remains incomplete. The WTK13 core captures ~500 kyr of climate variability, which includes one of these deep lake intervals, and our δD_{wax} should record both positive and negative changes in precipitation.

We calculated changes in the variance of our δD_{wax} and $\delta^{13}C_{wax}$ datasets using a moving, ~50-kyr window (n = 17 and 21 for δD_{wax} and $\delta^{13}C_{wax}$, respectively) to examine the relationship between environmental and insolation variability during the early Pleistocene (Fig. 7). This calculation does not require the variability in our record to be periodic. We observe a distinct peak in the variance of δD_{wax} and $\delta^{13}C_{wax}$ at ~1.73 Ma (139 mbs) associated with prominent positive and negative excursions in both δD_{wax} and $\delta^{13}C_{wax}$, suggesting this was a time interval marked by both much wetter and much drier conditions than average. We calculated the variance in different windows (from 100 to 18 kyrs), and found that the timing and amplitude of the increase in δD_{wax} variability at ~1.73 Ma (the maximum variance) is insensitive to the size of the moving window, suggesting the finding is robust.

The interval of high variability in our data corresponds to one of several intervals of high orbital eccentricity and insolation variability in our record. Moreover, the variability in δD_{wax} during this interval is significantly higher than that of the last 20 kyr, a time of low eccentricity that includes significant environmental change associated with the African Humid Period (Fig. 3; Morrissey, 2014). Despite the association between high eccentricity and δD_{wax} variance at ~1.73 Ma, other eccentricity maxima are not correlated with changes in the variance of δD_{wax} nor $\delta^{13}C_{wax}$, suggesting this time interval may have been uniquely sensitive to insolation forcing. There are various regional and global climatic changes that may contribute to this sensitivity, yet no one explanation is particularly robust. Indian Ocean SST oscillated dramatically at about this time

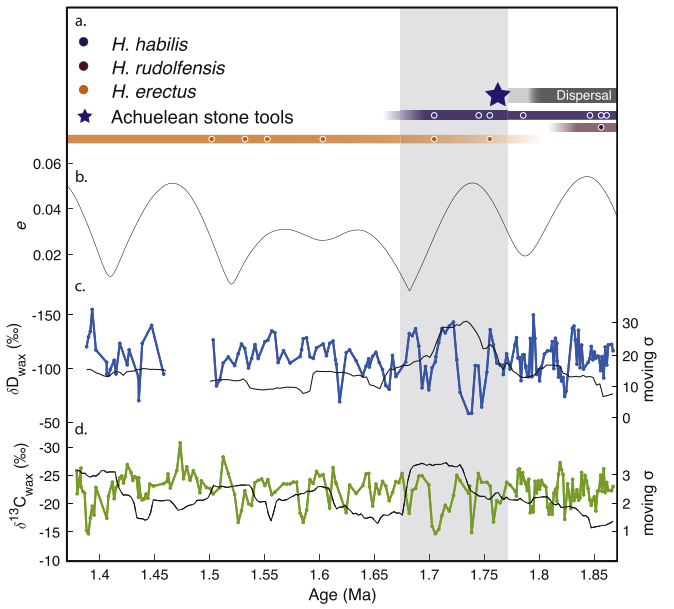

Fig. 7. δD_{wax} (c) and $\delta^{13}C_{wax}$ (d) from West Turkana with their moving standard deviations in black. The shaded region from 1.78 to 1.68 Ma shows higher variance in δD_{wax} and $\delta^{13}C_{wax}$ during an interval of high orbital eccentricity (b; Laskar et al., 2004). a) Hominin assemblages, as well as technological and biogeographic events in the West Turkana Basin. The time frame and environmental context of many evolutionary events are captured by the WTK13 drill core, including the extinctions of *H. habilis* (blue) and *H. rudolfensis* (purple), the speciation (orange) and dispersal out of Africa (grey) of *H. erectus*, and the appearance of Acheulean stone tools at 1.76 Ma (blue star). Circles denote real fossil dates, while the colored bands denote life span with faded regions referring to the error associated with first and last appearance dates, as well as uncertainties on dispersal time (Boaz and Howell, 1977; Wood and Leakey, 2011 and references therein). (For interpretation of the references to color in this figure legend, the reader is referred to the Web version of this article.)

(Herbert et al., 2010), and the Pacific Ocean zonal SST gradients began to increase between 1.8 and 1.7 Ma, marking the development of the strong Walker circulation that exists today (Wara et al., 2005). Ravelo et al. (2004) suggest that climate became more sensitive to insolation forcing after the onset of the Walker circulation due to the sensitivity and global hydroclimatic reach of the Walker circulation itself. This could explain why δD_{wax} variation is high in our record during the eccentricity maximum following, but not prior to, 1.78 Ma. Unfortunately, our record is poorly sampled due to low organic preservation 1.50–1.45 Ma during the next eccentricity maximum, making this difficult to test. However, the WTK13 record clearly demonstrates that increased variance in climate during this time interval occurred in the context of high eccentricity and insolation variability. Moreover, our record indicates strong intervals of drying as well as wetter conditions during this time period, suggesting a more variable, rather than generally wetter, climate during a time of high eccentricity.

6. Hominin evolution

Paleohydrological changes could affect hominin species by altering vegetation structure, habitat, and/or resource availability (Vrba, 1985). Alternatively, large lakes and dry valleys can act as physical barriers to human migration, whereas transitions between these two endmembers can enable population mixing, all of which could respond to precipitation changes and plausibly enhance evolutionary change (Maslin and Christensen, 2007; Trauth et al., 2010). Although first and last appearance dates contain great uncertainty, the interval of high variability in δD_{wax} (~1.77–1.67 Ma) in Lake Turkana overlaps with various hominin evolutionary transitions (Fig. 7). *H. rudolfensis* and *H. habilis* went extinct, while *H. erectus* appeared and later dispersed out of Africa (Antón, 2012; Antón et al., 2014; Feibel et al., 1989, 2009; Ferring et al., 2011; Gathogo and Brown, 2006; Joordens et al., 2013; Leakey et al., 2012; Potts et al., 2004; Spoor et al., 2007, 2015), suggesting potential links between hydroclimatic variations and hominin evolution. Indeed, a relatively high number of species occurred at this time as a result of increased species turnover from speciation and extinction (Foley, 2016).

Our paleoclimate record can contextualize these evolutionary transitions and test prominent hominin evolutionary hypotheses. The savanna hypothesis posits gradual evolutionary changes during a slow climate change over millions of years, but a lack of trend in our δD_{wax} is discordant with this hypothesis for the ~1.9–1.4 Ma interval. The larger body size of *H. erectus* is thought to have allowed migration and thereby continued access to resources during extreme climate shifts (Antón, 2012). *H. erectus* also had increased cranial capacity (Holliday, 2012; Pontzer, 2012), and new Acheulean stone tool technology was developed during this same interval (Lepre et al., 2011), both of which may have facilitated the development of more complex behaviors in response to a more variable environment. The turnover from *H. habilis* and *H. rudolfensis* to *H. erectus,* as well as the innovation of more advanced hand axes, thus suggests that the evolutionary transitions favored more adaptability, rather than one specific environment or climate. This analysis lends support to the variability selection hypothesis (Potts and Faith, 2015), which is consistent with the relationship between hominin evolution and regional climate offered by our observations of paleohydrology in the Turkana Basin.

7. Conclusions

Our new δD_{wax} reconstruction from West Turkana, Kenya allows us to investigate orbital-scale changes in East African paleohydrology from a key locus of the hominin fossil record in the early Pleistocene. African paleoclimate records show a clear transition from C_3- to C_4-dominated environments over the Plio-Pleistocene, but during the ~500 kyr interval we study our records show no statistically significant trends toward a drier environment in the Turkana Basin. Global climate drivers, such as ice volume and SST, also do not exhibit trends during this 500 kyr window. Time series spectral analyses of our untuned data indicate a relatively consistent ~20 kyr periodicity in δD_{wax}, consistent with orbital precession, and moving variance tests on δD_{wax} and $\delta^{13}C_{wax}$ demonstrate high variability at ~1.73 Ma, during a time of high orbital eccentricity. This evidence strongly suggests that changes in summer insolation are the primary factor driving early Pleistocene hydrologic change in this region.

The time interval from ~1.8 to 1.7 Ma is marked by extremely high amplitude hydrologic change that greatly exceeds the variance observed during the last ~20 kyr, including the well-known African Humid Period. Although we do not observe a consistent relationship between high eccentricity and high-amplitude variations in δD_{wax}, the ~1.8–1.7 Ma interval coincides with multiple shifts in the hominin fossil record in the Turkana Basin and the *H. erectus* dispersal out of Africa. We suggest that the rapid, extreme climate shifts may have driven these changes in fossil hominins towards enhanced adaptability.

Acknowledgements

We wish to thank Laura Messier for sample preparation, Rafael Tarozo for laboratory assistance, Sylvia Dee and Martin Trauth for assistance with statistical analyses, and the members of the

Hominin Sites and Paleolakes Drilling Project for useful discussions. Initial core processing and sampling were conducted at the US National Lacustrine Core Facility (LacCore) at the University of Minnesota. Thanks to the Kenyan National Council for Science and Technology and the Kenyan Ministry of Mines for research and export permits; the National Environmental Management Authority of Kenya for environmental drilling permits; DOSECC Exploration Services; Drilling and Prospecting International Ltd; the Nariokotome Mission and the people of Nariokotome. We would also like to thank Boniface Kimeu and Francis Ekai, and the members of the West Turkana science field team: Chris Campisano, Chad Yost, Sarah Ivory, Les Dullo, Tannis McCartney, Ryan O'Grady, Gladys Tuitoek, Elizabeth Kimburi, and Thomas Johnson. Support for HSPDP has been provided by the National Science Foundation (NSF) grants EAR 1123942, EAR 1338553, and BCS 1241859, the International Continental Scientific Drilling Program (ICDP), and the Institute at Brown for Environment and Society, Brown University (IBES). Data are freely available at the World Data Center-A for Paleoclimatology. We thank Kevin Uno and an anonymous reviewer for helpful comments on an earlier version of this manuscript. This is publication 11 of the Hominin Sites and Paleolakes Drilling Project.

Appendix A. Supplementary data

Supplementary data related to this article can be found at https://doi.org/10.1016/j.quascirev.2018.03.012.

References

Achyuthan, H., Quade, J., Roe, L., Placzek, C., 2007. Stable isotopic composition of pedogenic carbonates from the eastern margin of the Thar Desert, Rajasthan, India. Quat. Int. 162, 50–60.
Antón, S.C., 2012. Early Homo: who, when, and where. Curr. Anthropol. 53, S278–S298.
Antón, S.C., Potts, R., Aiello, L.C., 2014. Evolution of early Homo: an integrated biological perspective. Science 345, 1236828.
Blumenthal, S.A., Levin, N.E., Brown, F.H., Brugal, J.-P., Chritz, K.L., Harris, J.M., Jehle, G.E., Cerling, T.E., 2017. Aridity and hominin environments. Proc. Natl. Acad. Sci. Unit. States Am. 201700597.
Boaz, N.T., Howell, F.C., 1977. A gracile hominid cranium from upper member G of the Shungura formation, Ethiopia. Am. J. Phys. Anthropol. 46, 93–108.
Bobe, R., Behrensmeyer, A.K., 2004. The expansion of grassland ecosystems in Africa in relation to mammalian evolution and the origin of the genus Homo. Palaeogeogr. Palaeoclimatol. Palaeoecol. 207, 399–420.
Bray, E., Evans, E., 1961. Distribution of n-paraffins as a clue to recognition of source beds. Geochem. Cosmochim. Acta 22, 2–15.
Brierley, C.M., Fedorov, A.V., Liu, Z., Herbert, T.D., Lawrence, K.T., LaRiviere, J.P., 2009. Greatly expanded tropical warm pool and weakened Hadley circulation in the early Pliocene. Science 323, 1714–1718.
Brown, F., Feibel, C., 1991. Stratigraphy, depositional environments and palaeogeography of the Koobi Fora formation. Koobi Fora Res. Proj. 3, 1–30.
Butzer, K.W., Isaac, G.L., Richardson, J.L., Washbourn-Kamau, C., 1972. Radiocarbon dating of East African lake levels. Science 175, 1069–1076.
Campisano, C.J., Cohen, A.S., Arrowsmith, J.R., Asrat, A., Behrensmeyer, A.K., Brown, E.T., Deino, A.L., Deocampo, D.M., Feibel, C.S., Kingston, J.D., 2017. The hominin sites and paleolakes drilling project: high-resolution paleoclimate records from the east African rift system and their implications for understanding the environmental context of hominin evolution. PaleoAnthropology 2017, 1–43.
Cane, M.A., Molnar, P., 2001. Closing of the Indonesian seaway as a precursor to east African aridification around 3–4 million years ago. Nature 411, 157–162.
Carroll, A.R., Bohacs, K.M., 1999. Stratigraphic classification of ancient lakes: balancing tectonic and climatic controls. Geology 27, 99–102.
Cerling, T.E., 1992. Development of grasslands and savannas in East Africa during the Neogene. Palaeogeogr. Palaeoclimatol. Palaeoecol. 97, 241–247.
Cerling, T.E., Hay, R.L., 1986. An isotopic study of paleosol carbonates from Olduvai Gorge. Quat. Res. 25, 63–78.
Chikaraishi, Y., Naraoka, H., 2007. δ 13 C and δD relationships among three n-alkyl compound classes (n-alkanoic acid, n-alkane and n-alkanol) of terrestrial higher plants. Org. Geochem. 38, 198–215.
Cohen, A., Arrowsmith, R., Behrensmeyer, A.K., Campisano, C., Feibel, C., Fisseha, S., Johnson, R., Bedaso, Z.K., Lockwood, C., Mbua, E., 2009. Understanding paleoclimate and human evolution through the hominin sites and paleolakes drilling Project. Sci. Drill. 8, 60–65.
Cohen, A., Campisano, C., Arrowsmith, R., Asrat, A., Behrensmeyer, A., Deino, A., Feibel, C., Hill, A., Johnson, R., Kingston, J., 2016. The Hominin Sites and Paleolakes Drilling Project: inferring the environmental context of human evolution from eastern African rift lake deposits. Sci. Drill. 21, 1.
Costa, K., Russell, J., Konecky, B., Lamb, H., 2014. Isotopic reconstruction of the African humid period and Congo air boundary migration at Lake Tana, Ethiopia. Quat. Sci. Rev. 83, 58–67.
Dansgaard, W., 1964. Stable isotopes in precipitation. Tellus 16, 436–468.
Dart, R.A., 1925. In: Garwin, Laura, Lincoln, Tim (Eds.), Australopithecus Africanus: the Man-ape of South Africa. A Century of Nature: Twenty-one Discoveries that Changed Science and the World, pp. 10–20.
Deino, A.L., Kingston, J.D., Glen, J.M., Edgar, R.K., Hill, A., 2006. Precessional forcing of lacustrine sedimentation in the late Cenozoic Chemeron Basin, Central Kenya Rift, and calibration of the Gauss/Matuyama boundary. Earth Planet Sci. Lett. 247, 41–60.
deMenocal, P.B, 1995. Plio-pleistocene African climate. Science (New York, NY) 270, 53–59.
deMenocal, P.B, 2004. African climate change and faunal evolution during the Pliocene–Pleistocene. Earth Planet Sci. Lett. 220, 3–24.
Eglinton, G., Hamilton, R.J., 1967. Leaf epicuticular waxes. Science 156, 1322–1335.
Feakins, S.J., DeMenocal, P.B., Eglinton, T.I., 2005. Biomarker records of late Neogene changes in northeast African vegetation. Geology 33, 977–980.
Feibel, C.S., 2011. A geological history of the Turkana Basin. Evol. Anthropol. Issues News Rev. 20, 206–216.
Feibel, C.S., Brown, F.H., McDougall, I., 1989. Stratigraphic context of fossil hominids from the Omo Group deposits: northern Turkana Basin, Kenya and Ethiopia. Am. J. Phys. Anthropol. 78, 595–622.
Feibel, C.S., Lepre, C.J., Quinn, R.L., 2009. Stratigraphy, correlation, and age estimates for fossils from Area 123, Koobi Fora. J. Hum. Evol. 57, 112–122.
Ferring, R., Oms, O., Agustí, J., Berna, F., Nioradze, M., Shelia, T., Tappen, M., Vekua, A., Zhvania, D., Lordkipanidze, D., 2011. Earliest human occupations at Dmanisi (Georgian Caucasus) dated to 1.85–1.78 Ma. Proc. Natl. Acad. Sci. Unit. States Am. 108, 10432–10436.
Foley, R.A., 2016. Mosaic evolution and the pattern of transitions in the hominin lineage. Phil. Trans. R. Soc. B 371, 20150244.
Gao, L., Edwards, E.J., Zeng, Y., Huang, Y., 2014. Major evolutionary trends in hydrogen isotope fractionation of vascular plant leaf waxes. PLoS One 9, e112610.
Garcin, Y., Schwab, V.F., Gleixner, G., Kahmen, A., Todou, G., Séné, O., Onana, J.-M., Achoundong, G., Sachse, D., 2012. Hydrogen isotope ratios of lacustrine sedimentary n-alkanes as proxies of tropical African hydrology: insights from a calibration transect across Cameroon. Geochem. Cosmochim. Acta 79, 106–126.
Gasse, F., 2000. Hydrological changes in the African tropics since the last glacial maximum. Quat. Sci. Rev. 19, 189–211.
Gathogo, P.N., Brown, F.H., 2006. Revised stratigraphy of Area 123, Koobi Fora, Kenya, and new age estimates of its fossil mammals, including hominins. J. Hum. Evol. 51, 471–479.
Grove, M., 2014. Evolution and dispersal under climatic instability: a simple evolutionary algorithm. Adapt. Behav. 22, 235–254.
Grove, M., 2015. Palaeoclimates, plasticity, and the early dispersal of Homo sapiens. Quat. Int. 369, 17–37.
Harris, J., Brown, F., Leakey, M., 1988. Stratigraphy and paleontology of the Nachukui Formation, Lake Turkana region, Kenya. Contributions in science. Los Angel. Cty. Mus. Nat. Hist. 399, 1–128.
Herbert, T.D., Peterson, L.C., Lawrence, K.T., Liu, Z., 2010. Tropical ocean temperatures over the past 3.5 million years. Science 328, 1530–1534.
Hilgen, F., 1991. Astronomical calibration of Gauss to Matuyama sapropels in the Mediterranean and implication for the geomagnetic polarity time scale. Earth Planet Sci. Lett. 104, 226–244.
Holliday, T., 2012. Body size, body shape, and the circumscription of the genus Homo. Curr. Anthropol. 53 (suppl. 6), S330–S345. https://doi.org/10.1086/667360.
Hou, J., D'Andrea, W.J., Huang, Y., 2008. Can sedimentary leaf waxes record D/H ratios of continental precipitation? Field, model, and experimental assessments. Geochem. Cosmochim. Acta 72, 3503–3517.
Ivory, S.J., Russell, J., 2016. Climate, herbivory, and fire controls on tropical African forest for the last 60ka. Quat. Sci. Rev. 148, 101–114.
Joordens, J.C., Dupont-Nivet, G., Feibel, C.S., Spoor, F., Sier, M.J., van der Lubbe, J.H., Nielsen, T.K., Knul, M.V., Davies, G.R., Vonhof, H.B., 2013. Improved age control on early Homo fossils from the upper Burgi Member at Koobi Fora, Kenya. J. Hum. Evol. 65, 731–745.
Joordens, J.C., Vonhof, H.B., Feibel, C.S., Lourens, L.J., Dupont-Nivet, G., van der Lubbe, J.H., Sier, M.J., Davies, G.R., Kroon, D., 2011. An astronomically-tuned climate framework for hominins in the Turkana Basin. Earth Planet Sci. Lett. 307, 1–8.
Joseph, A., Frangi, J.P., Aranyossy, J.F., 1992. Isotope characteristics of meteoric water and groundwater in the Sahelo-Sudanese zone. J. Geophys. Res. Atmosphere 97, 7543–7551.
Kingston, J.D., Deino, A.L., Edgar, R.K., Hill, A., 2007. Astronomically forced climate change in the Kenyan Rift Valley 2.7–2.55 Ma: implications for the evolution of early hominin ecosystems. J. Hum. Evol. 53, 487–503.
Konecky, B., Russell, J., Bijaksana, S., 2016. Glacial aridity in central Indonesia coeval with intensified monsoon circulation. Earth Planet Sci. Lett. 437, 15–24.

Konecky, B.L., Russell, J.M., Johnson, T.C., Brown, E.T., Berke, M.A., Werne, J.P., Huang, Y., 2011. Atmospheric circulation patterns during late Pleistocene climate changes at Lake Malawi, Africa. Earth Planet Sci. Lett. 312, 318–326.
Larrasoaña, J., Roberts, A., Rohling, E., Winklhofer, M., Wehausen, R., 2003. Three million years of monsoon variability over the northern Sahara. Clim. Dynam. 21, 689–698.
Laskar, J., Robutel, P., Joutel, F., Gastineau, M., Correia, A., Levrard, B., 2004. A long-term numerical solution for the insolation quantities of the Earth. Astron. Astrophys. 428, 261–285.
Leakey, M.G., Spoor, F., Dean, M.C., Feibel, C.S., Antón, S.C., Kiarie, C., Leakey, L.N., 2012. New fossils from Koobi Fora in northern Kenya confirm taxonomic diversity in early Homo. Nature 488, 201–204.
Lepre, C.J., 2014. Early Pleistocene lake formation and hominin origins in the Turkana–Omo rift. Quat. Sci. Rev. 102, 181–191.
Lepre, C.J., Quinn, R.L., Joordens, J.C., Swisher, C.C., Feibel, C.S., 2007. Plio-Pleistocene facies environments from the KBS Member, Koobi Fora Formation: implications for climate controls on the development of lake-margin hominin habitats in the northeast Turkana Basin (northwest Kenya). J. Hum. Evol. 53, 504–514.
Lepre, C.J., Roche, H., Kent, D.V., Harmand, S., Quinn, R.L., Brugal, J.-P., Texier, P.-J., Lenoble, A., Feibel, C.S., 2011. An earlier origin for the Acheulian. Nature 477, 82–85.
Levin, N.E., Brown, F.H., Behrensmeyer, A.K., Bobe, R., Cerling, T.E., 2011. Paleosol carbonates from the Omo Group: isotopic records of local and regional environmental change in East Africa. Palaeogeogr. Palaeoclimatol. Palaeoecol. 307, 75–89.
Levin, N.E., Quade, J., Simpson, S.W., Semaw, S., Rogers, M., 2004. Isotopic evidence for plio–pleistocene environmental change at Gona, Ethiopia. Earth Planet Sci. Lett. 219, 93–110.
Levin, N.E., Zipser, E.J., Cerling, T.E., 2009. Isotopic composition of waters from Ethiopia and Kenya: insights into moisture sources for eastern Africa. J. Geophys. Res.: Atmosphere 114.
Lisiecki, L.E., Raymo, M.E., 2005. A Pliocene-Pleistocene stack of 57 globally distributed benthic δ18O records. Paleoceanography 20.
Lourens, L., Antonarakou, A., Hilgen, F., Van Hoof, A., 1996. Evolution of Plio-Pleistocene astronomical time scale. Paleoceanography 11, 391–413.
Maslin, M.A., Brierley, C.M., Milner, A.M., Shultz, S., Trauth, M.H., Wilson, K.E., 2014. East African climate pulses and early human evolution. Quat. Sci. Rev. 101, 1–17.
Maslin, M.A., Christensen, B., 2007. Tectonics, orbital forcing, global climate change, and human evolution in Africa: introduction to the African paleoclimate special volume. J. Hum. Evol. 53, 443–464.
Maslin, M.A., Trauth, M.H., 2009. Plio-pleistocene East African pulsed climate variability and its influence on early human evolution. Vertebr. Paleobiol. Paleoanthropol. Series 151.
Morrissey, A., 2014. Stratigraphic Framework and Quaternary Paleolimnology of the Lake Turkana Rift, Kenya. PhD Thesis. Syracuse University, Syracuse, NY, p. 188. Paper 62.
Morrissey, A., Scholz, C.A., 2014. Paleohydrology of lake Turkana and its influence on the Nile river system. Palaeogeogr. Palaeoclimatol. Palaeoecol. 403, 88–100.
Nicholson, S.E., 1996. A Review of Climate Dynamics and Climate Variability in Eastern Africa. The Limnology, Climatology and Paleoclimatology of the East African Lakes, pp. 25–56.
Otto-Bliesner, B.L., Russell, J.M., Clark, P.U., Liu, Z., Overpeck, J.T., Konecky, B., Nicholson, S.E., He, F., Lu, Z., 2014. Coherent changes of southeastern equatorial and northern African rainfall during the last deglaciation. Science 346, 1223–1227.
Owen, R., Barthelme, J.W., Renaut, R., Vincens, A., 1982. Palaeolimnology and archaeology of Holocene deposits north-east of lake Turkana, Kenya. Nature 298, 523–529.
Pokras, E.M., Mix, A.C., 1987. Earth's precession cycle and Quaternary climatic change in tropical Africa. Nature 326, 486–487.
Polissar, P.J., Freeman, K.H., 2010. Effects of aridity and vegetation on plant-wax δD in modern lake sediments. Geochem. Cosmochim. Acta 74, 5785–5797.
Pontzer, H., 2012. Ecological energetics in early Homo. Curr. Anthropol. 53 (suppl. 6), S346–S358. https://doi.org/10.1086/667402.
Potts, R., 1996. Evolution and climate variability. Science 273, 922.
Potts, R., 1998a. Environmental hypotheses of hominin evolution. Am. J. Phys. Anthropol. 107, 93–136.
Potts, R., 1998b. Variability selection in hominid evolution. Evol. Anthropol. Issues News Rev. 7, 81–96.
Potts, R., Behrensmeyer, A.K., Deino, A., Ditchfield, P., Clark, J., 2004. Small mid-Pleistocene hominin associated with East African Acheulean technology. Science 305, 75–78.
Potts, R., Faith, J.T., 2015. Alternating high and low climate variability: the context of natural selection and speciation in Plio-Pleistocene hominin evolution. J. Hum. Evol. 87, 5–20.
Ravelo, A.C., Andreasen, D.H., Lyle, M., Lyle, A.O., Wara, M.W., 2004. Regional climate shifts caused by gradual global cooling in the Pliocene epoch. Nature 429, 263–267.
Roche, H., Brugal, J.-P., Delagnes, A., Feibel, C., Harmand, S., Kibunjia, M., Prat, S., Texier, P.-J., 2003. Les sites archéologiques plio-pléistocènes de la formation de Nachukui, Ouest-Turkana, Kenya: bilan synthétique 1997–2001. Comptes Rendus Palevol 2, 663–673.
Rose, C., Polissar, P.J., Tierney, J.E., Filley, T., deMenocal, P.B., 2016. Changes in northeast African hydrology and vegetation associated with Pliocene–Pleistocene sapropel cycles. Philos. Trans. R. Soc. Lond. B Biol. Sci. 371.
Rossignol-Strick, M., 1985. Mediterranean Quaternary sapropels, an immediate response of the African monsoon to variation of insolation. Palaeogeogr. Palaeoclimatol. Palaeoecol. 49, 237–263.
Rozanski, K., Araguás-Araguás, L., Gonfiantini, R., 1993. Isotopic Patterns in Modern Global Precipitation. Climate Change in Continental Isotopic Records, pp. 1–36.
Sachse, D., Billault, I., Bowen, G.J., Chikaraishi, Y., Dawson, T.E., Feakins, S.J., Freeman, K.H., Magill, C.R., McInerney, F.A., Van Der Meer, M.T., 2012. Molecular Paleohydrology: Interpreting the Hydrogen-isotopic Composition of Lipid Biomarkers from Photosynthesizing Organisms.
Sachse, D., Radke, J., Gleixner, G., 2004. Hydrogen isotope ratios of recent lacustrine sedimentary n-alkanes record modern climate variability. Geochem. Cosmochim. Acta 68, 4877–4889.
Schefuß, E., Schouten, S., Schneider, R.R., 2005. Climatic controls on central African hydrology during the past 20,000 years. Nature 437, 1003–1006.
Scholl, M.A., Shanley, J.B., Zegarra, J.P., Coplen, T.B., 2009. The Stable Isotope Amount Effect: New Insights from NEXRAD Echo Tops. Luquillo Mountains, Puerto Rico. Water Resources Research 45.
Shanahan, T.M., McKay, N.P., Hughen, K.A., Overpeck, J.T., Otto-Bliesner, B., Heil, C.W., King, J., Scholz, C.A., Peck, J., 2015. The time-transgressive termination of the African Humid Period. Nat. Geosci. 8, 140–144.
Shultz, S., Maslin, M., 2013. Early human speciation, brain expansion and dispersal influenced by African climate pulses. PLoS One 8, e76750.
Sier, M.J., Langereis, C.G., Dupont-Nivet, G., Feibel, C.S., Joordens, J.C., van der Lubbe, J.H., Beck, C.C., Olago, D., Cohen, A., 2017. The top of the Olduvai subchron in a high-resolution magnetostratigraphy from the west Turkana core WTK13, hominin sites and paleolakes drilling Project (HSPDP). Quat. Geochronol.
Sonntag, C., Muennich, K., Junghans, C., Klitzsch, E., Thorweihe, U., Weistroffer, K., Loehnert, E., El-Shazly, E., Swailem, F., 1979. Palaeoclimatic information from deuterium and oxygen-18 in carbon-14-dated north Saharian groundwaters. Groundwater formation in the past. Isot. Hydrol. 1978.
Spoor, F., Gunz, P., Neubauer, S., Stelzer, S., Scott, N., Kwekason, A., Dean, M.C., 2015. Reconstructed Homo habilis type OH 7 suggests deep-rooted species diversity in early Homo. Nature 519, 83–86.
Spoor, F., Leakey, M.G., Gathogo, P.N., Brown, F.H., Antón, S.C., McDougall, I., Kiarie, C., Manthi, F.K., Leakey, L.N., 2007. Implications of new early Homo fossils from Ileret, east of Lake Turkana, Kenya. Nature 448, 688–691.
Thomas, E.K., Huang, Y., Morrill, C., Zhao, J., Wegener, P., Clemens, S.C., Colman, S.M., Gao, L., 2014. Abundant C 4 plants on the Tibetan plateau during the lateglacial and early Holocene. Quat. Sci. Rev. 87, 24–33.
Tierney, J.E., Russell, J.M., Damsté, J.S.S., Huang, Y., Verschuren, D., 2011. Late quaternary behavior of the east African monsoon and the importance of the Congo air boundary. Quat. Sci. Rev. 30, 798–807.
Trauth, M.H., 2015. MATLAB Recipes for Earth Sciences, 4 ed. Springer-Verlag Berlin Heidelberg.
Trauth, M.H., Larrasoaña, J.C., Mudelsee, M., 2009. Trends, rhythms and events in Plio-Pleistocene African climate. Quat. Sci. Rev. 28, 399–411.
Trauth, M.H., Maslin, M.A., Deino, A., Strecker, M.R., 2005. Late cenozoic moisture history of East Africa. Science 309, 2051–2053.
Trauth, M.H., Maslin, M.A., Deino, A.L., Junginger, A., Lesoloyia, M., Odada, E.O., Olago, D.O., Olaka, L.A., Strecker, M.R., Tiedemann, R., 2010. Human evolution in a variable environment: the amplifier lakes of Eastern Africa. Quat. Sci. Rev. 29, 2981–2988.
Trauth, M.H., Maslin, M.A., Deino, A.L., Strecker, M.R., Bergner, A.G., Dühnforth, M., 2007. High-and low-latitude forcing of Plio-Pleistocene East African climate and human evolution. J. Hum. Evol. 53, 475–486.
Uno, K.T., Polissar, P.J., Jackson, K.E., deMenocal, P.B., 2016a. Neogene biomarker record of vegetation change in eastern Africa. Proc. Natl. Acad. Sci. Unit. States Am. 113 (23), 6355–6363.
Uno, K.T., Polissar, P.J., Kahle, E., Feibel, C., Harmand, S., Roche, H., deMenocal, P.B., 2016b. A Pleistocene palaeovegetation record from plant wax biomarkers from the Nachukui Formation, West Turkana, Kenya. Philos. Trans. R. Soc. Lond. B Biol. Sci. 371.
Vogts, A., Moossen, H., Rommerskirchen, F., Rullkötter, J., 2009. Distribution patterns and stable carbon isotopic composition of alkanes and alkan-1-ols from plant waxes of African rain forest and savanna C 3 species. Org. Geochem. 40, 1037–1054.
Volkman, J.K., Barrett, S.M., Blackburn, S.I., Mansour, M.P., Sikes, E.L., Gelin, F., 1998. Microalgal biomarkers: a review of recent research developments. Org. Geochem. 29, 1163–1179.
Vrba, E.S., 1980. Evolution, species and fossils-how does life evolve. South Afr. J. Sci. 76, 61–84.
Vrba, E.S., 1985. Environment and evolution: alternative causes of the temporal distribution of evolutionary events. South Afr. J. Sci. 81, 229–236.
Vrba, E.S., 1989. Levels of selection and sorting with special reference to the species level. Oxf. Surv. Evol. Biol. 6, 111–168.
Vrba, E.S., 1995. On the Connections between Paleoclimate and Evolution. Paleoclimate and Evolution, with Emphasis on Human Origins, pp. 24–45.
Vuille, M., Werner, M., Bradley, R.S., Chan, R., Keimig, F., 2005. Stable isotopes in East African precipitation record Indian Ocean zonal mode. Geophys. Res. Lett. 32.
Wara, M.W., Ravelo, A.C., Delaney, M.L., 2005. Permanent El Niño-like conditions during the Pliocene warm period. Science 309, 758–761.
Wood, B., Leakey, M., 2011. The Omo-Turkana Basin fossil hominins and their contribution to our understanding of human evolution in Africa. Evol. Anthropol. Issues News Rev. 20, 264–292.

Yang, W., Seager, R., Cane, M.A., Lyon, B., 2015. The annual cycle of East African precipitation. J. Clim. 28, 2385–2404.
Yuretich, R.F., Cerling, T.E., 1983. Hydrogeochemistry of Lake Turkana, Kenya: mass balance and mineral reactions in an alkaline lake. Geochem. Cosmochim. Acta 47, 1099–1109.
Zachos, J., Pagani, M., Sloan, L., Thomas, E., Billups, K., 2001. Trends, rhythms, and aberrations in global climate 65 Ma to present. Science 292, 686–693.